Chirality-glass and spin-glass correlations in the two-dimensional random-bond XY model

P. Ray and M. A. Moore
Department of Theoretical Physics, The University, Manchester M13 9PL, United Kingdom
(Received 20 September 1991; revised manuscript received 10 December 1991)

The nearest-neighbor XY spin-glass model on square lattices with both Gaussian and random $\pm J$ bond distributions has been studied by Monte Carlo simulations and the results analyzed by finite-size scaling methods. For both bond distributions, we find a power-law divergence of the spin-glass correlation length, $\xi \sim T^{-\nu}$, as $T \to 0$, with $\nu \simeq 1$. The exponent η, which describes the decay of correlations at zero temperature, is $\simeq 0$ for the Gaussian bond distribution, but for $\pm J$ bonds, η attains a small positive value ~ 0.15, implying that the ground state is highly degenerate. The chiral degrees of freedom also exhibit glass ordering as $T \to 0$, with the chiralities ordered randomly without any spatial periodicity. The correlation-length exponent ν_c corresponding to the chiral glass ordering as $T \to 0$ is $\simeq 2$ for both kinds of bond distribution. The different values obtained for ν and ν_c suggest that there may be two distinct correlation lengths associated with this zero-temperature phase transition.

I. INTRODUCTION

In recent years there has been much interest in frustrated planar-spin systems because of their very close analogies with arrays of Josephson junctions in a magnetic field. It was pointed out by Villain[1] that frustrated XY spin systems have two kinds of symmetry: the usual continuous O(2) symmetry associated with the global rotational invariance of the Hamiltonian and a discrete symmetry associated with the invariance of the Hamiltonian under a reflection of the planar spins about an arbitrary direction. This discrete symmetry is manifested through the chiralities of the plaquettes that are flipped by the reflection-symmetry operation (see Ref. 2, for example). A precise definition of chirality is given below in Eq. (11) (but see also Ref. 3). Chirality can be regarded as the sign of the magnetic moment produced by the current flowing around the plaquette in the Josephson-junction analog. For an isolated frustrated plaquette, there are two degenerate ground-state orientations for the spins. One ground state is associated with a clockwise-spin rotation as one travels around the plaquette, and the other ground state with a counterclockwise rotation, the handedness determining the chirality of the ground state. Thus an isolated frustrated plaquette can be associated with an Ising-like up-down symmetry.

Numerical studies[4,5] of the fully frustrated XY model show that it has a phase transition at a finite temperature T_c. Long-range chiral order is observed in the low-temperature phase. The transition is most unusual in that there seem to be two diverging correlation lengths as $T \to T_c$. One correlation length depends on temperature in the manner predicted for the XY ferromagnet by Kosterlitz[6] and is associated with the continuous symmetry O(2), while the other is associated with the discrete Ising symmetry and has a temperature dependence similar to that of the two-dimensional Ising model.

However, unlike the fully frustrated case, little is known about the situation where there is quenched random disorder in the system and when, instead of being uniformly frustrated, the system is frustrated randomly as a consequence of the disorder. In such systems Villain[1] has discussed the possibility of a chiral ordering of the spin-glass type—the chiral glass. A Monte Carlo study by Kawamura and Tanemura[7] of the spin-glass and chiral-glass susceptibilities for the two-dimensional $\pm J$ XY spin glass indicated that both had a power-law divergence of the form $\chi \sim T^{-\gamma}$, as $T \to 0$, with the susceptibility exponent γ for the spin degrees of freedom estimated to be 1.9 ± 0.1, while that for the chiral variables was determined to be larger than 4.5.

In this paper we present further results of Monte Carlo simulations on the two-dimensional XY spin glass with short-range interactions and in the absence of any external magnetic field. We have studied both the $\pm J$ and Gaussian distribution for the bonds. For both distributions the spin-glass susceptibility seems to diverge as $T \to 0$. Our finite-size scaling results imply a power-law divergence of the spin-glass correlation length $\xi \sim T^{-\nu}$ as $T \to 0$, and we estimate the exponents ν and η which describe this transition. We find that $\nu \simeq 1.0$ for both distributions, a value consistent with those obtained previously.[8,9] For the Gaussian distribution $\eta \simeq 0$, but for the $\pm J$ case, η attains a small value $\simeq 0.15$. This implies that the $\pm J$ case has a high ground-state degeneracy. The chiral-glass correlations are harder to analyze as the scaling regime for them seems to occur only at rather low temperatures where data points from the Monte Carlo simulation can be obtained for relatively small systems. The data points suggest a power-law divergence of the chiral-glass correlation length $\xi_c \sim T^{-\nu_c}$, with $\nu_c \simeq 2.0$, for both bond distributions. This implies that, as in the uniformly frustrated case, the randomly frustrated XY spin glass may have also two distinct correlation lengths simultaneously present in the system. Again, the two correlation lengths correspond to the continuous and chiral degrees of freedom, but for the randomly frustrated XY model, they are associated with a zero-temperature transition. Kawamura and Tanemura[12] have recently reached the same con-

clusion from a domain-wall renormalization-group analysis.

II. MODEL AND SCALING ANALYSIS

We consider the XY spin glass described by the Hamiltonian

$$H=-\sum_{\langle ij\rangle} J_{ij}\cos(\theta_i-\theta_j)\ , \tag{1}$$

where θ_i is the angle of orientation of the planar spin at site i of a square lattice and the sum is taken over nearest-neighbor pairs $\langle ij\rangle$. The exchange interactions J_{ij} are independent random variables taken from either the distribution

$$P(J_{ij})=\tfrac{1}{2}[\delta(J_{ij}-1)+\delta(J_{ij}+1)]\ ,$$

known as the $\pm J$ distribution, or

$$P(J_{ij})=\frac{1}{\sqrt{2\pi}}\exp(-J_{ij}^2/2)\ , \tag{2}$$

the Gaussian distribution. Temperature is always given in units of the root-mean-square nearest-neighbor interaction.

The scaling analysis follows that given by Bhatt and Young.[10] There is only one independent static exponent if $T_c=0$, and the ground state is nondegenerate (aside from states related by a continuous rotation or a reflection). If the ground state is highly degenerate, one more exponent, η, is needed to describe the transition. Other exponents can be determined from these through scaling relations. We study the spin-autocorrelation function

$$q(t)=\frac{1}{N}\left[\sum_i \cos[\theta_i(t_0)-\theta_i(t_0+t)]\right]_{\rm av}\ , \tag{3}$$

where $\theta_i(t)$ is the angle of the planar spin at site i and time t, and N is the total number of spins in the system. Here $(\cdots)_{\rm av}$ indicates an average over the bond distribution. Thermal averages have been replaced by time averages, as is generally done in Monte Carlo simulations. The time t_0 should be greater than the relaxation time of the system. For any finite system, $q(t)\to 0$ as $t\to\infty$. Another important quantity is the four-spin-correlation function

$$Nq^2(t)=\frac{1}{N}\left[\left[\sum_i \cos[\theta_i(t_0)-\theta_i(t_0+t)]\right]^2\right]_{\rm av}\ , \tag{4}$$

which provides an estimate of the spin-glass susceptibility

$$\chi_{\rm SG}=\frac{1}{N}\left[\sum_{i,j}\langle\cos(\theta_i-\theta_j)\rangle^2\right]_{\rm av}\ , \tag{5}$$

in the large-t limit. Here $\langle\cdots\rangle$ denotes the thermal average. $\chi_{\rm SG}$ for an $L\times L$ system has the finite-size scaling form[10]

$$\chi_{\rm SG}(L,T)=L^{2-\eta}f((T-T_c)L^{1/\nu})\ , \tag{6}$$

where L is the linear size of the lattice and f is the scaling function. The exponents η and ν can be determined by collapsing the data onto the scaling form as given by Eq. (6). However, since this involves three unknown parameters T_c, η, and ν, the collapse of all the data on to a single curve is not straightforward.

It is therefore particularly useful to look at the dimensionless parameter[11]

$$u=\frac{q^4(t)}{[q^2(t)]^2}\ , \tag{7}$$

in the limit $t\to\infty$, where

$$q^4(t)=\frac{1}{N_4}\left[\left[\sum_i \cos[\theta_i(t_0)-\theta_i(t_0+t)]\right]^4\right]_{\rm av}\ . \tag{8}$$

In the paramagnetic phase where $L\gg\xi$, q will have a Gaussian distribution and $u=3$. At $T=0$ the spin configurations at two different times may differ by a global spin rotation or belong to different degenerate states. If rotations are the only spin changes possible, $u=(\langle\cos^4\theta\rangle)_{\rm av}/[(\langle\cos^2\theta\rangle)_{\rm av}]^2=\frac{3}{2}$. The degeneracy which arises from reflections, i.e., $\theta_i\to\phi-\theta_i$, for arbitrary ϕ, affects the value of u by an amount which decreases as $1/N$. We define the renormalized coupling constant

$$g(L,T)=\tfrac{2}{3}(3-u)\ , \tag{9}$$

which will then vary from $g=0$ at high temperature to $g=1$ at $T=0$, provided there is no extensive ground-state degeneracy and N is large. The variation of g is given by the finite-size scaling ansatz[11]

$$g(L,T)=\bar{g}((T-T_c)L^{1/\nu})\ , \tag{10}$$

where $\bar{g}$ is a scaling function. This scaling form involves only one exponent ν. Equation (10) implies that $g(L,T)$ at $T=T_c$ is independent of L, so that all the curves for different L should intersect at T_c. For $T>T_c$, $g(L,T)$ is a decreasing function of L, whereas for $T<T_c$ it is an increasing function of L, becoming a step function at $T=T_c$ in the limit $L\to\infty$. A reliable estimate of T_c can then be obtained from the point where all the curves intersect each other. Once T_c is determined, ν is fixed by finding which value for it makes all the data for different L and T best fit the scaling form given by Eq. (10). The scaling form [Eq. (6)] for the spin-glass susceptibility can be then used to obtain the exponent η.

For the chiral variables, we proceed in the same way as for the spins. Chirality k is the handedness of the spins at the corners of an elementary plaquette. At a plaquette α, the chirality k_α is defined by[3]

$$k_\alpha=\mathrm{sgn}\left[\sum_{\langle ij\rangle} J_{ij}\sin(\theta_i-\theta_j)\right]\ , \tag{11}$$

where the summation is taken over a directed closed path along the sides of the plaquette. For the ground state of a single isolated frustrated plaquette, the chirality defined in the above way assumes the value 1 or -1.

We define the autocorrelation function of the chiral variables as

$$r(t)=\frac{1}{N'}\left[\sum_\alpha k_\alpha(t_0)k_\alpha(t_0+t)\right]_{\rm av}\ , \tag{12}$$

where $k_\alpha(t)$ is the chirality of the plaquette α at the time t and the summation is over all the plaquettes. N' denotes the total number of plaquettes in the system. k_α behaves like pseudo-Ising spins and in the long-time limit $r(t)\to 0$ because of the sampling of states in the limit which are related by reflection and which cause the chiralities to flip. Higher moments of $r(t)$, defined by

$$r^n(t)=\frac{1}{(N')^n}\left[\left[\sum_\alpha k_\alpha(t_0)k_\alpha(t_0+t)\right]^n\right]_{\rm av}, \tag{13}$$

have been studied. The chiral susceptibility is then defined as $\chi_c=N'r^2(t)$. We define the dimensionless parameter

$$v=\frac{r^4(t)}{[r^2(t)]^2}, \tag{14}$$

which will vary from 3 in the paramagnetic phase at high temperature to 1 at zero temperature (in the absence of degeneracy effects). The analog of $g(L,T)$ for the chiral case is

$$g_c(L,T)=\tfrac{1}{2}(3-v), \tag{15}$$

which behaves similarly to $g(L,T)$ and obeys the finite-size scaling ansatz of Eq. (10). The transition temperature and chiral correlation-length exponent ν_c can then be determined in the same way.

III. NUMERICAL METHOD

Our numerical procedures closely follow those of Bhatt and Young.[10] The time-dependent overlap $q(t)$ and $r(t)$ and their higher moments are determined for planar spins situated at the sites of an $L\times L$ square lattice. Periodic boundary conditions are used so that $N=N'$. The system is simulated for t_0 time steps, and the overlap is then determined by simulating the system for a further t steps. Each time step corresponds to one Monte Carlo step per spin. t_0 and t should be large compared with the equilibriation time of the system. In practice, we make $t=t_0$ and compute $q^n(t_0)$ or $r^n(t_0)$ by taking the overlap between the t_0th value of the respective quantities to the $(2t_0+\tau)$th value of the same and then averaging over successive τ_0 number of observations:

$$q^n(t_0)=\left[\frac{1}{\tau_0}\sum_{\tau=1}^{\tau_0}\left[\frac{1}{N}\sum_i\cos[\theta_i(t_0)-\theta_i(2t_0+\tau)]\right]^n\right]_{\rm av},$$
$$r^n(t_0)=\left[\frac{1}{\tau_0}\sum_{\tau=1}^{\tau_0}\left[\frac{1}{N}\sum_\alpha k_\alpha(t_0)k_\alpha(2t_0+\tau)\right]^n\right]_{\rm av}. \tag{16}$$

We have varied τ_0 from 5000 to 10 000 steps, depending on the size and temperature of the system. We have to use bigger values of τ_0 for the larger L values and the lower temperatures T.

The value of t_0 is chosen to remove effects due to nonequilibriation of the system. To fix its value, we again follow Bhatt and Young[10] and calculate the mutual overlap between spins or chiralities from two identical copies of the system θ_i^1 and θ_i^2 with the same realization of the bonds. At any temperature the two systems are simulated in parallel for t_0 steps and the instantaneous mutual overlaps for both the spins and chiralities are then determined for successive τ_0 steps. We thereby get the replica-averaged values (denoted by the subscript r) of the quantities $q^n(t_0)$ and $r^n(t_0)$:

$$q_r^n(t_0)=\left[\frac{1}{\tau_0}\sum_{\tau=1}^{\tau_0}\left[\frac{1}{N}\sum_i\cos[\theta_i^1(t_0+\tau)-\theta_i^2(t_0+\tau)]\right]^n\right]_{\rm av},$$
$$r_r^n(t_0)=\left[\frac{1}{\tau_0}\sum_{\tau=1}^{\tau_0}\left[\frac{1}{N}\sum_\alpha k_\alpha^1(t_0+\tau)k_\alpha^2(t_0+\tau)\right]^n\right]_{\rm av}, \tag{17}$$

where $k_\alpha^1(t)$ and $k_\alpha^2(t)$ are the chiralities of the plaquette α in the two systems 1 and 2 at time t. In the case when t_0 is sufficiently large and the system reaches its equilibrium state, $q^n(t_0)$ or $r^n(t_0)$ becomes equal (within the limits of statistical error) to $q_r^n(t_0)$ and $r_r^n(t_0)$, respectively. Obviously, t_0 will depend on the system size L and temperature T and varied from 3000 for small L and high T to as much as 75 000 for large L and low T. We could not go to much lower temperatures because of the difficulties in equilibriation. For the $\pm J$ bonds, the lowest temperature that could be attained was $T=0.25$ for $L=6$, 8, and 10 and $T=0.275$ for $L=12$ and only 0.3 for $L=16$. The equilibriation difficulties also restrict us to the maximum size $L=16$. For the Gaussian bond distribution, the maximum size simulated was $L=10$, and for the smaller system sizes, we could go to temperatures as low as $T=0.15$. To perform bond averaging, 150–300 different bond configurations were generated for each of the distributions.

IV. RESULTS

The scaling form of $g(L,T)$ and $g_c(L,T)$ as given in Eq. (10) suggests that the curves for different L and T should intersect each other at $T=T_c$. Figures 1 and 2 show the data for $g(L,T)$ for various values of L and for

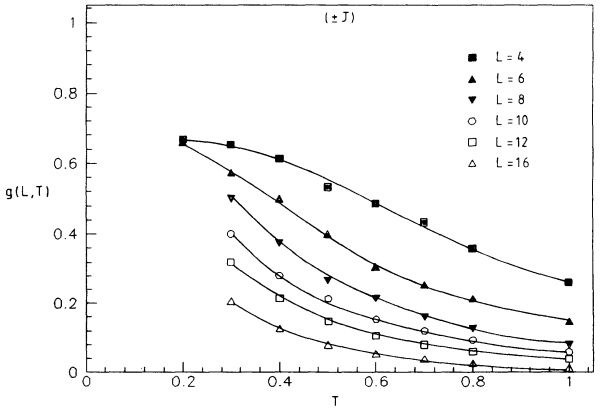

FIG. 1. Plot of $g(L,T)$ against T for various lattice sizes for the $\pm J$ distribution. The lines are guides to the eye.

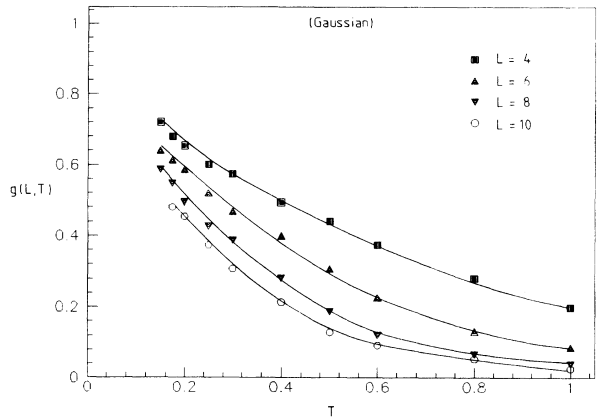

FIG. 2. Plot of $g(L,T)$ against T for various lattice sizes for the Gaussian distribution. The lines are guides to the eye.

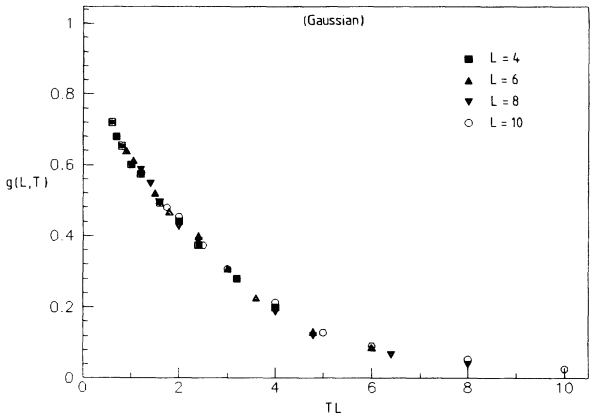

FIG. 4. Scaling plot of $g(L,T)$ against $(T-T_c)L^{1/\nu}$, with $T_c=0$ and $\nu=1.0$, for the Gaussian distribution.

$\pm J$ and Gaussian bond distributions, respectively. In both the figures, curves for different L values seem to meet each other only at $T=0$. This behavior is precisely what is expected at a zero-temperature transition. In Fig. 1, for the $\pm J$ bond distribution, the values of g for different L, instead of heading toward unity, seem to attain a saturation value which is less than unity and remain constant as the temperature is lowered. Though we could not go to very low temperature, especially for larger system sizes, the nature of the curves in Fig. 1 is strongly reminiscent of the behavior that is expected in the presence of high ground-state degeneracy in the system (see Ref. 10). This feature is absent in Fig. 2 for the Gaussian bond distribution, where all the curves are directed toward unity at $T=0$.

Scaling plots for $g(L,T)$ against $TL^{1/\nu}$ are given in Figs. 3 and 4 for the $\pm J$ and Gaussian distributions, respectively. From Eq. (10) all the data should collapse onto the same curve if T_c and ν are chosen properly. We find this occurs with $T_c=0$ and $\nu=1.0\pm0.06$ for both distributions. The error bars associated with the exponent values are the estimates that demarcate the region beyond which the quality of the collapse deteriorates, given the statistical errors. They do not, however, allow for any systematic errors which may occur due to corrections to scaling, etc.

The spin-glass susceptibility $\chi_{SG}(L,T)$ for $\pm J$ and Gaussian bond distributions are shown in Figs. 5 and 6 and their scaling plots in Figs. 7 and 8, respectively. The susceptibility data support the scaling relation as is given by Eq. (6) with $T_c=0$ and $\nu=1.0$. However, for the $\pm J$ case, we find that a small value of $\eta\simeq0.15\pm0.05$ improves the collapse, while for the Gaussian case the best value is $\eta\simeq0$. The finite value of η for the $\pm J$ model indicates the presence of high degeneracy in the ground state of the model, resulting in a power-law decay of the correlations at $T=0$, whereas for the Gaussian distribution there is a unique ground state (up to rotations and reflections), and so η should be zero.

For the chiralities we present the curves for $g_c(L,T)$ in Figs. 9 and 10 for both bond distributions. Unlike those for the spins, $g_c(L,T)$ remains small down to quite low temperatures and then increases sharply. The increase of $g_c(L,T)$ at low temperature indicates the buildup of chiral correlations. However, as for the spin-correlation case, we have not found any indication of a finite-temperature transition. All the curves for $g_c(L,T)$ for different L values seem to converge to unity only at $T=0$. The curves of $g_c(L,T)$ for the $\pm J$ and Gaussian distributions are very similar to one another, unlike for the spin

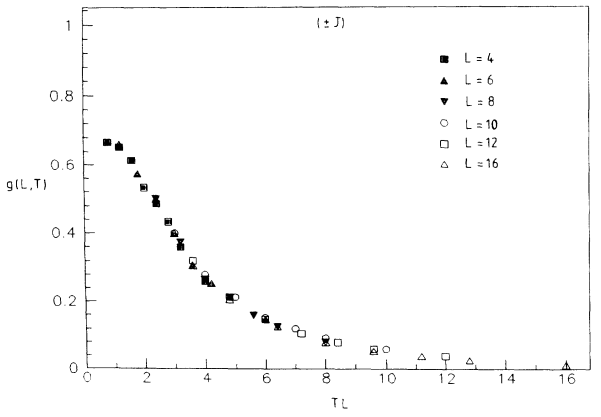

FIG. 3. Scaling plot of $g(L,T)$ against $(T-T_c)L^{1/\nu}$, with $T_c=0$ and $\nu=1.0$, for the $\pm J$ distribution.

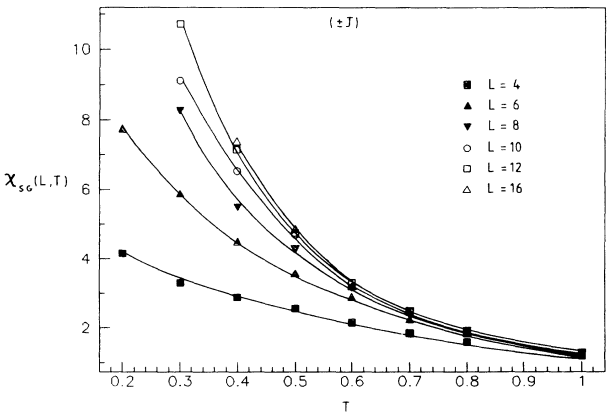

FIG. 5 Plot of $\chi_{SG}(L,T)$ against T for various lattice sizes for the $\pm J$ distribution. The lines are guides to the eye.

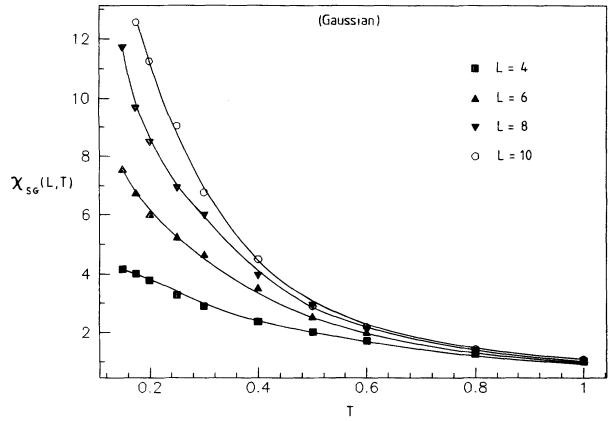

FIG. 6. Plot of $\chi_{SG}(L,T)$ against T for various lattice sizes for the Gaussian distribution. The lines are guides to the eye.

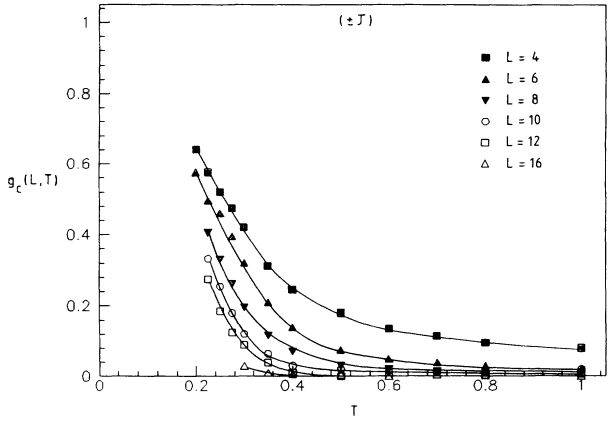

FIG. 9. Plot of $g_c(L,T)$ against T for various lattice sizes for the $\pm J$ distribution. The lines are guides to the eye.

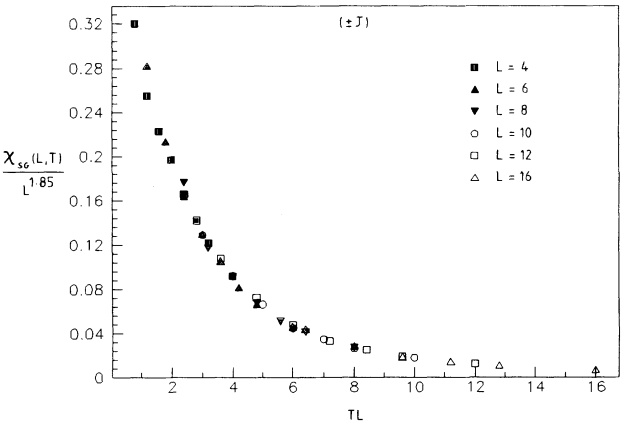

FIG. 7. Scaling plot of $\chi_{SG}(L,T)/L^{(2-\eta)}$ against $(T-T_c)L^{1/\nu}$, with $T_c=0$ $\nu=1.0$, and $\eta=0.15$, for the $\pm J$ distribution.

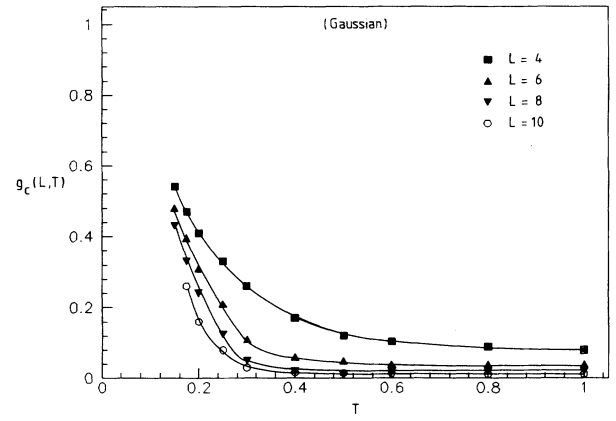

FIG. 10. Plot of $g_c(L,T)$ against T for various lattice sizes for the Gaussian distribution. The lines are guides to the eye.

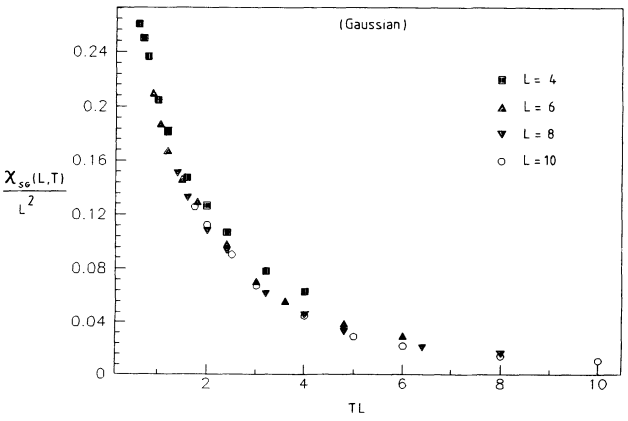

FIG. 8. Scaling plot of $\chi_{SG}(L,T)/L^{(2-\eta)}$ against $(T-T_c)L^{1/\nu}$, with $T_c=0$, $\nu=1.0$, and $\eta=0.0$, for the Gaussian distribution.

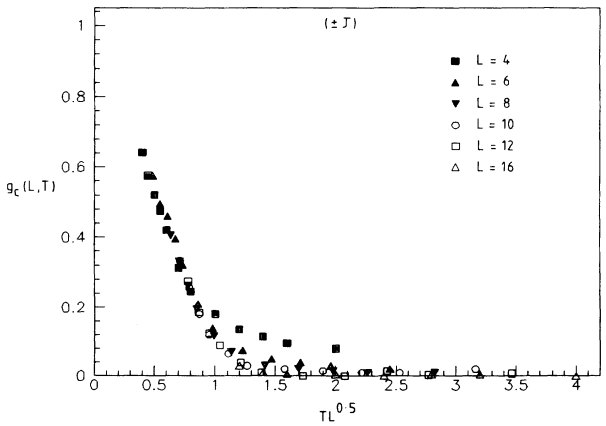

FIG. 11. Scaling plot of $g_c(L,T)$ against $(T-T_c)L^{1/\nu_c}$, with $T_c=0$ and $\nu_c=2.0$, for the $\pm J$ distribution.

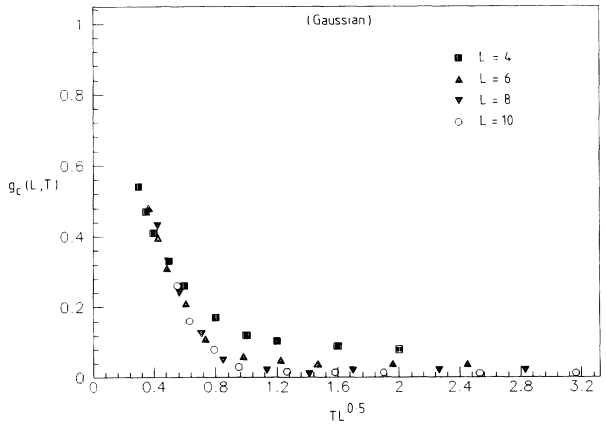

FIG. 12. Scaling plot of $g_c(L,T)$ against $(T-T_c)L^{1/\nu_c}$, with $T_c=0$ and $\nu_c=2.0$, for the Gaussian distribution.

case, indicating that the degeneracies of the ground state for $\pm J$ bonds have less consequence for g_c. The scaling plots for $g_c(L,T)$ against TL^{1/ν_c} are shown in Figs. 11 and 12 for the $\pm J$ and Gaussian cases, respectively. We see that the data obey the scaling relation given by Eq. (10) with $T_c=0$ and $\nu_c=2.0\pm0.15$ for both bond distributions. The high-temperature data show systematic deviations away from collapsing to a single curve, presumably because these data are not in the scaling regime, whereas for the spin plots, data at the same temperature lay in the scaling regime. The chiral susceptibility remains flat down to a quite low temperature and then increases sharply. The larger the system size, the sharper is the increase of susceptibility. The scaling of the susceptibility data is, however, not good, as only a few points are found in the scaling regime.

V. CONCLUSION

We have carried out a Monte Carlo study of both the $\pm J$ and Gaussian XY spin glasses on square lattices with nearest-neighbor interactions. Finite-size scaling analyses were used to understand the results for different lattice sizes from $L=4$ to 16. We find that the results are consistent with a spin-glass transition only at temperature $T=0$. A power-law divergence of the spin-glass correlation length $\xi\sim T^{-\nu}$ as $T\to0$ was found with $\nu\simeq1.0$ for both distributions, in agreement with earlier estimates.[8,9] For the $\pm J$ distribution, the results indicate the existence of high ground-state degeneracy leading to a power-law decay of the correlation at $T=0$ described by the exponent η, which we estimate as $\eta=0.15$. In fact, a large number of degenerate states have been directly observed in a separate simulation of the $\pm J$ bond system, where in each step of the simulation the spins were orientated in the directions of the internal field at their respective sites until no further change was possible. Degeneracies have been observed for lattice sizes as large as 20×20. However, at this stage, we do not fully understand the origin of the degeneracy. The spin-glass susceptibility exponent γ can be obtained through the scaling relation $\gamma=(2-\eta)\nu=1.85$, which agrees well with the estimate of Jain and Young[8] and Kawamura and Tanemura.[7]

An important aspect of our work has been the study of the behavior of the chiral degrees of freedom. In the case of the uniformly frustrated XY system, there are two correlation lengths, one XY like, driven by the spins and the other Ising like, mediated by the chiral degrees of freedom (see Ref. 5 and references therein). We find that in the XY spin glass, which is randomly frustrated, there also apparently exist two length scales in the system corresponding to the spin and chiral degrees of freedom. The chiralities exhibit a glass transition at zero temperature simultaneously with the spins. There is no sign of any finite-temperature transition. However, we would like to mention that, because of the unavailability of very-low-temperature data, a transition at very low temperature cannot be ruled out. We have found a power-law divergence of the chiral correlation length as $T\to0$ with an exponent $\nu_c\simeq2.0$ for both the $\pm J$ and Gaussian bond distributions. The exponent values indicate that the spin- and chiral-glass transitions belong to different universality classes and suggest that there are two distinct correlation lengths associated with the zero-temperature transition in the XY spin-glass systems. Unlike for the spin case, we do not find any indication of the effects of ground-state degeneracy for the chiral variables. We would like to stress that the number of low-temperature data points in the scaling regime for the chiral-glass correlations are rather few, and at this stage the suggestion of two correlation lengths should really be accepted with reservation. Kawamura and Tanemura[12] have recently reported domain-wall renormalization-group studies of chiral ordering in the $\pm J$ XY spin glass in both two and three dimensions. In both dimensions they also find evidence for the presence of two different correlation lengths in the system, corresponding to the spin and chiral degrees of freedom. For two dimensions they obtain $\nu=1.2\pm0.15$ and $\nu_c=2.6\pm0.3$, which are slightly higher than those estimated by us. However, it should be observed that if extensive degeneracy is present for the $\pm J$ model, as we believe, then the distribution function for the domain-wall energy would not achieve a fixed shape, which makes the analysis for ν_c and ν somewhat problematic.[13] Kawamura and Tanemura[12] report that in three dimensions there is evidence for a finite-temperature chiral-glass transition, but with no XY spin-glass ordering—a most intriguing situation.

ACKNOWLEDGMENTS

We should like to thank A. J. Bray, S. Murphy and J. M. Kim for useful discussions. One of us (P.R.) thanks the SERC for financial support.

[1]J. Villain, J. Phys. C **10**, 1717 (1977); **10**, 4793 (1977).
[2]D. S. Fisher and D. A. Huse, Phys. Rev. B **38**, 386 (1988).
[3]E. Fradkin, B. Huberman, and S. H. Shenker, Phys. Rev. B **18**, 4789 (1978).
[4]S. Teitel and C. Jayaprakash, Phys. Rev. Lett. **51**, 1999 (1983); Phys. Rev. B **27**, 598 (1983); S. Miyashita and H. Shiba, J. Phys. Soc. Jpn. **53**, 1145 (1984); D. B. Nicolaides, J. Phys. A **24**, L231 (1991).
[5]E. Granato, J. M. Kosterlitz, J. Lee, and M. P. Nightingale, Phys. Rev. Lett. **66**, 1090 (1991).
[6]J. M. Kosterlitz, J. Phys. C **7**, 1046 (1974).
[7]H. Kawamura and M. Tanemura, Phys. Rev. B **36**, 7177 (1987).
[8]S. Jain and A. P. Young, J. Phys. C **19**, 3913 (1986).
[9]B. W. Morris, S. G. Colborne, M. A. Moore, A. J. Bray, and J. Canisius, J. Phys. C **19**, 1157 (1986).
[10]R. N. Bhatt and A. P. Young, Phys. Rev. B **37**, 5606 (1988).
[11]K. Binder, Z. Phys. B **43**, 119 (1981).
[12]H. Kawamura and M. Tanemura, J. Phys. Soc. Jpn. **60**, 608 (1991).
[13]M. A. Moore and S. Murphy (unpublished).